JWPU
Journal of Al-Wataniya Private University
ISSN: 3105-2150

Volume (3) Number (2)
Available at: https://doi.org/10.5281/zenodo.20962108

Evaluation of the Effect of Vibratory Compaction on the Propagation of vibrations in soil: A Comprehensive Analytical Study

Dr. Darien Ahmad [1,*]

ABSTRACT

Dynamic compaction by vibratory compaction is considered one of the most powerful and widely used soil improvement techniques in ~~the~~ practical engineering applications. However, this method generates vibrations which propagate through the surrounding soil in the form of different types of ground waves.

This research presents a numerical study using the finite element method to analyze the propagation of vibrations generated by dynamic compaction using vibratory compaction. Therefore, we propose a suitable numerical model that depends on the simulation of both the compaction force and the propagation site by using the software ABAQUS.

We validated the model using field measurements taken from previous studies, then we applied it to a typical example to study the propagation and damping of the vibrations caused by vibro-probe.

The results of the study allow the evaluation of the amplitude of vibrations at different distances, thus, assessing the probable effects and then taking appropriate mitigation measures.

KEYWORDS: dynamic compaction, ground waves, damping of vibrations, finite element method, ABAQUS.

Submitted on June 5, 2025; Revised on June 21, 2025; Accepted on July 4, 2025

1 Faculty of Civil Engineering, Al-Wataniya Private University, Hama, Syria.

* Corresponding author. E-mail address: darien-ahmad@wpu.edu.sy

1. Introduction

Dynamic compaction by vibro-probe is a type of deep compaction used to improve ~~the~~ thick deposits of loose and cohesive soils. Compaction generally increases soil density and the bearing capacity while reducing settlement and liquefaction potential. [1][2].

The vibrating probe consists of a vibrating unit, which is about 3 m long and is carried on a mechanical crane and has various shapes Figure (1). The vibrating unit contains an eccentric mass that creates a centrifugal force and causes vibration in the horizontal direction. There are openings in the top and base of the vibrating unit for water injection.

Thus, the vibrating probe increases the bearing capacity of loose soils by applying a vibrating force in successive vibratory impulses on the surface and in the lower layers.

FIGURE (1): DYNAMIC COMPACTION USING A VIBRATING PROBE.

Despite the many advantages of this method, one of the negative aspects that should not be overlooked is that it generates vibrations that spread in the soil surrounding the compaction area in the form of ground waves. These waves can cause damage to neighboring structures and disturb people in the vicinity if the compaction site is close to buildings and facilities. Therefore, this technique must be used with caution especially when the construction site is located in an urban area. In such cases, it is essential to predict the vibration amplitudes that may occur at different points within the soil before stating the compaction process. This allows engineers to assess ~~the~~

potential impacts on nearby people and structures and to take the appropriate preventive measures before actually starting the compaction process.

Volume waves propagate through the soil mass and are classified into two main types:

- Primary or compression waves (P) which are associated with a change in volume that causes alternating tension and compression of the soil. During their passage, they cause soil particles to vibrate in the direction parallel to the wave propagation path (Figure 2.a)
- Secondary or shear waves (S) which are accompanied by soil particles vibrating in the direction perpendicular to the wave propagation path without a change in volume (Figure 2.b).

The compression wave velocity (C_P) and shear wave velocity (CS) in a homogeneous elastic soil are given as follows:m

$$C_P = \sqrt{\frac{E(1-\mu)}{\rho(1+\mu)(1-2\mu)}} \qquad (1)$$

$$C_S = \sqrt{\frac{E}{2\rho(1+\mu)}} \qquad (2)$$

E :Soil elasticity modulus (Young's modulus) (kPa)

μ: Poisson's coefficient of soil.

ρ :Volumetric weight (t/m^3).

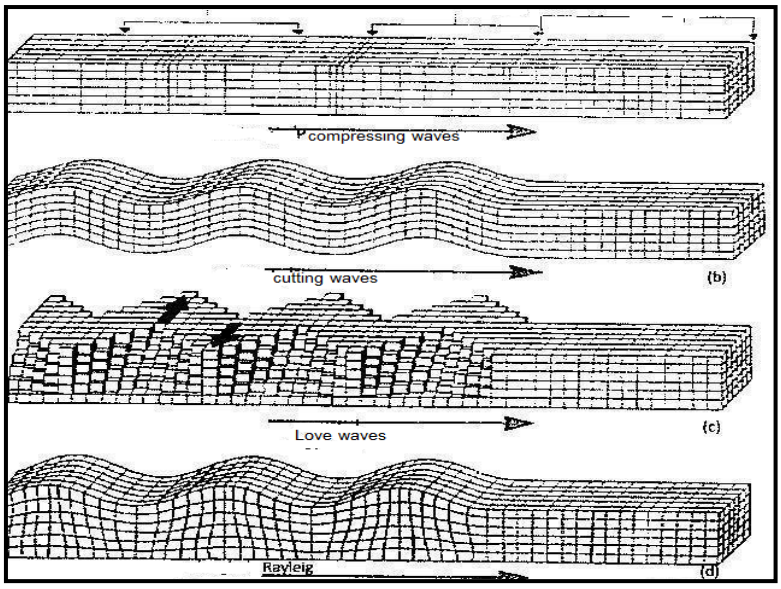

FIGURE (2): TYPES OF VIBRATIONAL WAVES.

Surface waves propagate at a limited depth near the surface of the earth (up to a depth approximately equal to the wavelength) and their propagation can be likened to the propagation of waves on the surface of a still lake when a stone is thrown into it. Two main types of surface waves can be distinguished:

- Love Waves (L) which cause soil points to move in the plane tangent to the soil surface perpendicular to the direction of their propagation (Figure 2.c). They do not cause shear deformations.
- Rayleigh Waves (R) which are the most common type of surface waves. They are accompanied by horizontal and vertical movement (elliptical movement) of soil particles similar to the movement of sea foam on the carrier wave (Figure 2.d), and lead to compressive (tensile) deformations in addition to shear deformations.

R waves propagate at a speed slightly less than C_S according to the relation:

$$C_R = \frac{0.87 + 1.12\nu}{1+\nu} C_S \cong (0.87 - 0.96)C_S \qquad (3)$$

The resulting waves lose their energy during their propagation, and thus their amplitude decreases with increasing distance from the compaction point. This phenomenon is called vibration damping, which is generally divided into two basic types: material damping and geometrical damping. Geometrical damping, which is independent of soil properties, is due to the increase in the wave front during its propagation; and thus, the energy is spread over a larger volume. Geometrical damping is generally expressed by the following relation [3]:

$$V_2 = V_1 \left(\frac{r_1}{r_2}\right)^n \qquad (4)$$

Where V_1 and V_2 represent the amplitude of the vibrations at distances r_1 and r_2 from the source respectively, and n is the geometric damping coefficient. The value of the coefficient n depends on the type of the propagating wave, the position of the vibration source and the distance between the vibration source and the vibration measurement point. Table (1) shows the proposed theoretical values of the coefficient n:

Table (1): values of the coefficient n [4]

Vibration source location	Type vibration wave	measurement point position	Coefficient value n
Point on the surface	R Suface wave	surface	0.5
Point on the surface	Volumetric wave	surface	2
Deep point	Volumetric wave	surface	1
Deep point	Volumetric wave	deep	1

Physical damping is the process of damping movement and vibration, and fading the amplitude of movement over time is related to the soil properties and results from the soil viscosity and internal friction between its particles. It is expressed by the factor α (1/m) called the "physical damping factor" whose value is related to the type of soil. Table (2) shows suggested theoretical values for the factor α according to the type of soil:

Table (2): Classification of soils according to the physical damping factor α[3]

Soil type	α (1/m) Material damping factor		Soil category
	50 Hz	5 Hz	
Loose soil ($N_{SPT} < 5$)	0,3−0,1	0,03−0,01	I
Well-tolerant soil ($5 < N_{SPT} < 15$)	0,1−0,03	0,01−0,003	II
solid soil ($15 < N_{SPT} < 50$)	0,03−0,003	0,003−0,0003	III
Well-tolerant solid soil ($50 < N_{SPT}$)	<0,003	< 0,0003	IV

Physical damping is linked to geometric damping and expressed together by the following relationship:

$$W_r = W_0 . e^{-\alpha(r-r_0)} \qquad (5)$$

W_r: Vibration wave energy at a measurement point located at a distance r from the vibration source.
W_0: Vibration wave energy at the point of source
r: Distance of measurement point from reference point.
r_0: Distance of the vibration source from the reference point.
α: physical damping factor.

Knowing the amplitude of vibrations at a certain distance from the vibration source is essential to anticipate their potential effects on soil, people and nearby structures. For this reason, before the actual application of the dynamic load, an attenuation relationship (vibration amplitude - distance from the source) must be found or established, taking into account both the type of dynamic vibration source to be applied and the specifications and conditions of the site soil. Such a relationship is found in several ways, the most important of which are:
- Field Experimental Method: It is the best and most reliable method, in which the true damping relationship is experimentally established on site. This method depends on using a vibration source that sends vibrations similar to the true source and measuring the vibration amplitude at three or four points located in a straight line on the ground surface and then drawing the actual damping curve passing through these points, which can be used to predict the vibration amplitude at any other intermediate point. Despite the high accuracy of this method, it may not be possible to apply practically in some cases, such as the case of the vibration source being located in a populated residential location where there is no available empty space to place the initial measurement points.
- Experimental-theoretical method: In this method, the amplitude of vibrations is predicted by means of experimental damping relations that have been established based on field measurements previously conducted in cases similar to the case to be studied or theoretical damping relations that have been derived from the general wave equation. An example of experimental relations can be mentioned as the following relation:

$$PPV = (\frac{153}{r})^{1.7} \quad (6)$$

PPV: Maximum molecular velocity of vibration (permissible limit value) (mm/sec)
r: Distance from impact point (contact) (m)
Attention should be paid to the specificity of such a relationship when used to predict vibrations, as it can give incorrect results when used for a location other than the original location for which the relationship was developed.
As for the theoretical damping relationships, the most widespread and widely used is the Bortenize relationship, named after the scientist who developed it in 1931, which is written in the form:

$$V_b = V_a (\frac{r_a}{r_b})^n e^{\alpha(r_a - r_b)} \quad (7)$$

V_a: Amplitude of vibrations at distances r_a and r_b from the source ($r_a > r_b$) & V_b
n: Engineering damping coefficient
α: Material damping coefficient.
It should be noted that this equation represents a solution to the wave equation for a single-phase wave with a constant frequency propagating in homogeneous soil, which practically limits the accuracy of its use due to the presence of multiple waves with different frequencies. However, it remains the most widespread relationship because it takes into account both the physical and geometric damping in the soil on the one hand, and gives results close to reality provided that the type of dominant wave is determined from among the different waves propagating in the soil on the other hand, we relied on this relationship in this study.
-Numerical method: It is the most effective method as it depends on the use of numerical methods such as the Finite Difference Method and the Finite Element Method, which allows for a detailed study and in-depth analysis of the phenomenon of wave propagation not only on the surface of the soil but also within it. It also allows for a parametric study of the factors affecting the amplitude of vibrations propagated in the soil.

2. Importance of research and its objectives

In recent years, interest has increased in dynamic compaction with a vibrating probe because it is an effective technique for increasing the soil bearing capacity, improving its properties, and reducing its tendency to sink to great depths, especially for coarse and loose soils.
However, most of the existing studies on the compaction process and the resulting vibration waves have focused mainly on evaluating the effectiveness of compaction and determining the area affected by compaction under and near the vibrating probe, while either neglecting or only briefly addressing the propagation of vibrations in the soil at distances away from the compaction point. [8],[7],[6],[5].
Therefore, the importance of this research stems from the scarcity of detailed studies on vibrations resulting from dynamic soil compaction, despite the importance of the subject.

In this study, a relatively simple yet effective numerical model is developed and validated which can be used before implementing compaction to predict the different types of vibration waves that will be generated and track their propagation in the soil. This allows the prediction of the amplitude of vibrations at each point in the soil and the adoption of appropriate mitigation measures when required to reduce their potential impact on people and neighboring facilities.
In addition, through the parametric study conducted, the most important factors affecting the amplitude of vibrations resulting from dynamic compaction with a vibrating rod were identified, as well as the nature of the influence. This contributes to improving the compaction process and enables better control of the resulting vibration levels.

3. Research methodology

In our study, we relied on the use of the finite element method to model the problem of vibration propagation resulting from dynamic compaction of soil using a vibrating probe. First, we developed a suitable numerical model for the problem based on modeling both the compaction force and the soil and implemented it into the finite element calculation software ABAQUS.
The model was then validated using field measurements results obtained from previous reference research. After validation, the model was used to conduct a numerical study in the time domain of the resulting vibrations. This analysis yielded important results related to:

- The types of vibration waves generated,
- their damping behavior,
- and the most important factors affecting their amplitude.

4. Numerical model

4.1. Modeling of the compaction force

The numerical study of dynamic soil compaction by vibrating probe method first requires modeling the compaction force applied to the soil. Based on previous studies, the vibrator used in compaction by vibrating -rod method produces a centrifugal compaction force F_v which acts vertically on the top of the probe and its maximum intensity is related to the frequency of the vibrator according to the following relation (8):

$$F_V = \xi_v \varpi^2 \qquad (8)$$

where

Centrifugal force intensity $(kN)\ F_V$:

$(\varpi = 2\pi f)$ angular frequency of the vibrator ϖ :

$(kN.m)_{\ v}$: Static moment ξ

There are curves showing the relationship between the properties of the vibrator (frequency-static torque) and the intensity of the centrifugal force generated by it. Figure (3).

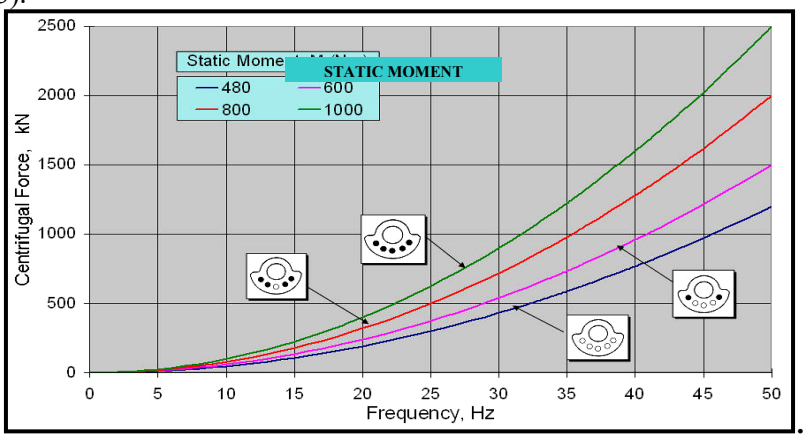

FIGURE (3) : DIAGRAM SHOWING THE FORCE GENERATED BY THE ROTATION OF THE PROBE [8]

This dynamic force is applied in the model as a pressure force acting on the upper end of the probe, which has a total length Lp and is embedded in the soil over a length LR [9][10].

The centrifugal force is modeled using a force-time function in the form of a sinusoidal wave, as shown in Figure (4) and expressed by the following relationship [11]:

$$F_{(t)} = F_V \sin(2\pi ft) \qquad (9)$$

F_v: Vibration frequency in soil.

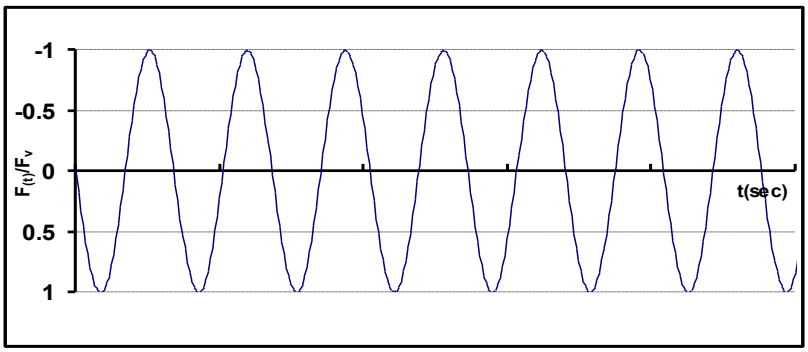

FIGURE (4): FORCE-TIME DIAGRAM OF DYNAMIC FORCE GENERATED BY THE VIBRATOR [8].

4.2. Finite element method

The finite element formulation of the relationships governing the interaction between the soil and the vibrating probe leads to the following set of equations:

$$[M]\{\ddot{u}\}+[C]\{\dot{u}\}+[K]\{u\}=\{F\} \qquad (10)$$

mass matrix $[M]$:

Damping matrix. $[C]$:

stiffness matrix $[K]$:

Ray of external forces acting on the nodes of the finite element network $\{F\}$:

Transmission rays, velocity, and molecular acceleration at network nodes :. $\{\ddot{u}\},\{\dot{u}\},\{u\}$

Soil damping is taken into account using Rayleigh's viscous damping formula, in which the damping matrix is formed as a linear combination of both the stiffness matrix and the mass matrix according to the following formula [12]. :

$$[C]=\alpha_M[M]+\alpha_K[K] \qquad (11)$$

These coefficients depend on the damping properties of the material. a_M, a_k :

This form of the damping matrix leads to the representation of damping in terms of the damping ratio, which is the sum of two componants: the first is directly proportional to the angular frequency of the vibration ω , while the second is inversely proportional to it according to the relation.:

$$\xi_i = \frac{\alpha_M}{2\omega_i} + \frac{\alpha_K \omega_i}{2} \qquad (12)$$

ξ_i: The damping ratio for vibration mode No *i* varies according to the nature of the soil, its layers, and the surrounding medium. It usually ranges between (5-10%) in matters of the propagation of elastic waves in the soil.

4.3. Spatial and temporal division

4.3.1. SPATIAL DIVISION STANDARD (Δx)

The spatial partitioning criterion is a delicate balance between accuracy and computational efficiency and its determination requires a deep understanding ~~of~~ the behavior of the object under loading, the principles of stress-strain analysis, and the constraints of the finite element software used.

The choice of finite element dimensions is very important to ensure the correct representation of the propagation of vibration waves in the soil. In general, it is recommended to use a finite element grid with a maximum dimension not exceeding the ratio (λmin/10) where λmin is the minimum wavelength (corresponding to the slowest wave, typically the surface wave R) [13] Accordingly, the finite element size was selected based on the following relation:

$$\Delta x \leq \frac{\lambda_R}{10} : \lambda_R = \frac{C_R}{f} \qquad (13)$$

Where C_R: is the propagation velocity of Rayleigh surface waves, and f is the frequency of vibrations.

Where Δx represents the minimum dimension of the network elements and C_P represents the velocity of the fastest wave propagation (pressure wave P).

4.3.2. TIME DIVISION CRITERION (OPTIONAL) (Δt)

Time stepping in numerical modeling in civil engineering is the process of dividing time into successive smaller time intervals, whereby the state of a system (such as a structure or soil) is calculated at each interval based on the state of the previous interval. This allows the simulation of system behavior over time, especially in cases where loads or conditions change with time.

The time step for calculation must be chosen carefully in order to ensure the accuracy of the solution. Reference [11] provides the following practical relation ***for*** selecting the time step Δt*:*

$$\frac{1}{10}\frac{\Delta x}{C_P} \leq \Delta t \leq \frac{\Delta x}{C_P} \qquad (14)$$

$$Ttotal \geq \frac{x}{C_R}$$

X: length of the soil model in which the study is conducted.

C_P: velocity the fastest propagating wave.

4.3.3. USED CONDITIONS

The probe was assumed to be composed of a homogeneous, isotropic, linear elastic material with negligible damping, while the soil behaviour was assumed to be linear elastic with Rayleigh viscous damping.

The probe and the surrounding soil were divided into four linear finite elements, and the calculation was carried out assuming axial symmetry about a vertical axis passing through the center of the probe.

The friction between the sides of the probe and the surrounding soil was considered to be completely of « Tie » type in ABAQUS, which means that the motion of the probe and the surrounding soil are identical, i.e. the relative motion between them is zero.

This assumption represents a conservative case, in which the greatest transfer of compaction energy to the surrounding soil occurs in the form of vibration waves[14] [**15**].

In order to avoid the phenomenon of reflection of waves propagating on the model boundaries, the model dimensions L*H were chosen to be sufficiently large to avoid interference of waves reflected on the model's lateral and lower boundaries with waves propagating within the time window considered in the analysis.

The model dimensions were selected based on the longest wavelength, ensuring that shorter wavelength is properly captured.

As for the model's boundray peripheral conditions, they are shown in the figure (5).

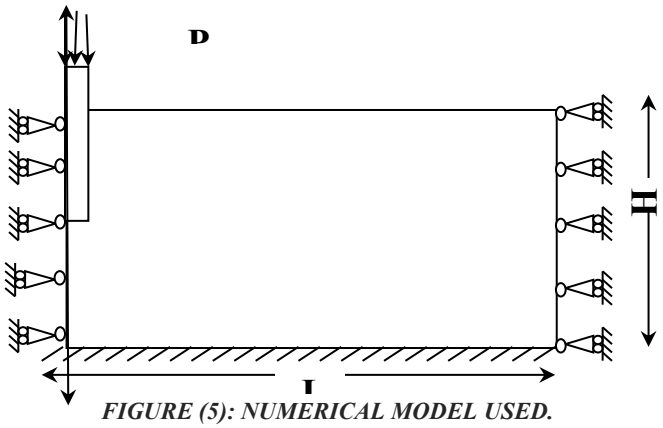

7

FIGURE (5): NUMERICAL MODEL USED.

4.4. Parameters required for modeling

The model used for modeling requires specifying spatial Δx and temporal partitioning parameters Δt , in addition to necessary parameters related to both the vibrating probe and the soil, which can be summarized as follows:

Vibrating- rod parameters: total length of the probe L , length of the part embedded in the soil L_R , radius of the vibrating probe r_0 , maximum centrifugal force generated by the vibrating probe F_V , vibrating frequency f .

Probe material parameters: modulus of elasticity of the probe material E_R , Poisson's modulus u_R , its bulk mass ρ_R .

Soil property parameters: Young's modulus E , Poisson's modulus μ , damping ratio ζ , bulk mass of the soil ρ .

5. Model Parameters

We will conduct a numerical study in the time and frequency domains of ~~the~~ vibrations resulting from dynamic compaction using the vibrating probe method. The study of the propagation of vibration waves in the compacted soil includes the following main points:

- Analysis of the types of vibration waves, their propagation, and their attenuation for a typical case.
- Parametric study of the most important factors affecting ~~the~~ vibrations resulting from dynamic soil compaction using the probe-vibrator method

- **Model used**

A typical example is defined as a soil domain with given dimensions $(60 * 60)$, in which soil improvement is carried out using a vibrating probe. The properties of both the soil and the vibrating probe are defined by the following parameters:

Table (3): parameter of model

Soil parameters	Vibro-rod parameters	model parameters
$E = 5MPA$ $\rho = 1.8t/m^3$ $\mu = 0.25$ $\zeta = 5\%$	height $L = 10m$ Length of the part embedded in the soil $L_R = 6m$ diameter $r_{r0} = 400mm$ $E_R = 210GPa$ $\rho_R = 7.8t/m3$ $u_R = 0.3$	$(60*60)$ $\Delta x = 0.15m$ $\Delta t = 0.0026\sec$ $\zeta = 5\%$ $\alpha_M = 4.7$ $\beta_M = 0.0005$

Based on the previous analysis, vibratory probe compaction generates a dynamic force in the form of a continuous sinusoidal function, which is applied in the numerical model as a uniformly distributed pressure load. This load varies sinusoidally with time and is distributed over a surface with a radius equal to that of the vibrating probe as shown in diagram (3)

The effective pressure load corresponding to the type of probe used at a frequency of $f = 15Hz$

$$p = \frac{240000}{\pi 0.2^2} = 1910828N/m^2$$

The soil mass is discretized using a square finite element grid, and the spatial discretization step is selected Δx.

– Δx :

$$\lambda = 27.7/15 = 1.88m$$

$$\Rightarrow \Delta x \le \frac{\lambda}{10} = 0.18 \Rightarrow \Delta x = 0.15m$$

– Δt :

$$\Delta t \le \frac{0.15}{57.7} = 0.0026 \Rightarrow \Delta t = 0.0026\sec$$

$$T_{total} \le 30/27.7 = 1\sec$$

-Damping ratio :

$$\zeta = 5\%$$

$$\alpha_M = 4.7$$

$$\beta_M = 0.0005$$

Assuming that the typical soil section has the dimensions shown in Figure (6) and by performing the calculation using a numerical program, the vibration values at all points of the finite element grid of the soil mass are obtained, the tracking of the generation, propagation and attenuation of waves in the soil.

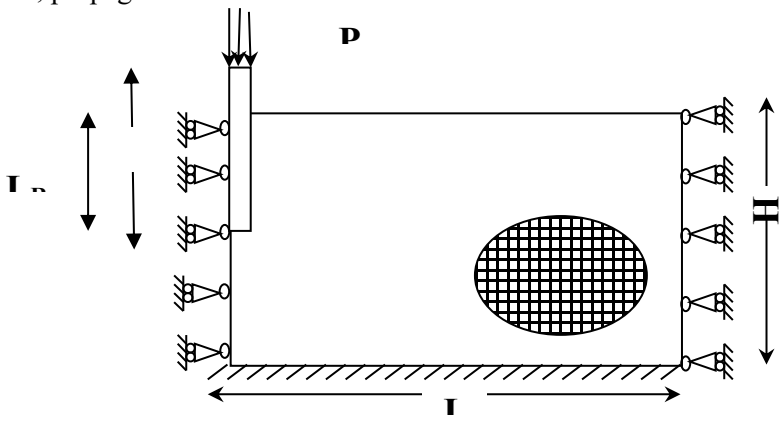

FIGURE (6) : TYPICAL EXAMPLE USED TO STUDY DYNAMIC COMPACTION USING THE VIBRO-ROD METHOD

The attenuation curves of both the vertical and horizontal components of the calculated vibration amplitudes on the soil surface were calculated at various distances from the vibration source, starting from a distance of r=9m. This study is distinguished by its focus on the vibration amplitudes at points relatively far from the vibrating probe, whereas most previous studies have focused on the effectiveness of the compaction in immediate vicinity of the compaction area, as shown in ~~the~~ figure (7).

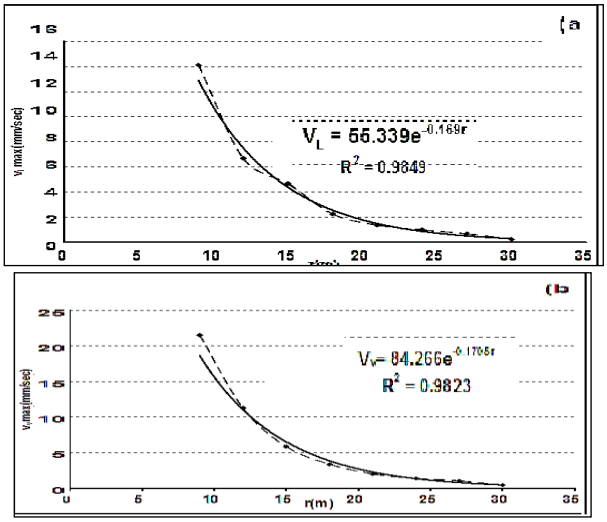

FIGURE (7) : DAMPING CURVES FOR VIBRATIONS CALCULATED AT THE SOIL SURFACE.

(A HORIZONTAL VEHICLE V_L (B VERTICAL VEHICLE V_V

From the figure, the following observations can be made :

- In the case of homogeneous soil compaction, the vibrations amplitudes in the vertical direction are greater than those in the horizontal direction.
- The amplitude of both the horizontal and vertical vibration components decrease with increasing distance from the compaction point. The mathematical analysis shows that this attenuation can be expressed by the following simplified damping relationship with a very high coefficient of determination *R* :

$$V_{MAX} = A.E^{-B.R} \qquad (14)$$

Where a and *b* are two numerical coefficients, the first is related to the vibration amplitude near the source (i. e., at a small distance from the center of vibration), and the second represents the overall damping (geometric and material) of vibrations.
To determine the dominant wave types in the time signals of the calculated vibrations at the soil surface (in both the horizontal and vertical directions), the attenuation was compared with three attenuation curves Figure (8)) derived from the Portenez relation (Equaion (**7**)), considering n=0.5 ،n=1 و n=2. The comparison assumes a given material damping factor, soft soil conditions, and a vibration frequency of 15 Hz. Figure (8) illustrates the comparison results:

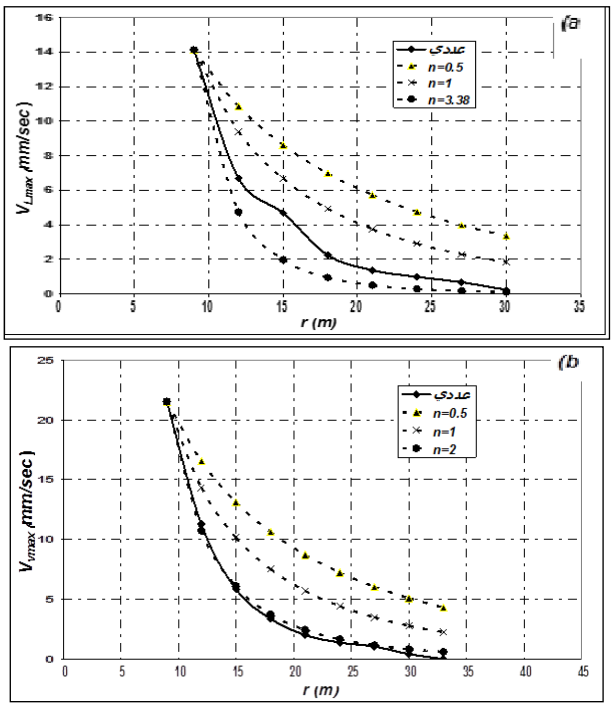

FIGURE (8) : CALIBRATION OF THE PORTENEZ DAMPING EQUATION ON THE NUMERICAL DAMPING CURVE WITH VARYING VALUES OF THE GEOMETRIC DAMPING FACTOR N ($A=0.04M^{-1}$).

(A HORIZONTAL VEHICLE V_L (B VERTICAL VEHICLE V_V

From this figure, it can be concluded that the length of the total time signal for the calculated vibrations is proportionally shorter than (1/r2) or n=2, which indicates a

volume wave propagating on the surface of the soil (according to Table 1). Therefore, the dominant waves in the horizontal and vertical directions are volume waves P.
In order to clarify the effect of physical damping, the damping curve of each of the two compounds was compared with the three damping curves calculated based on the Portenez relation while neglecting physical damping (α=0). The results are presented in Figure (9).

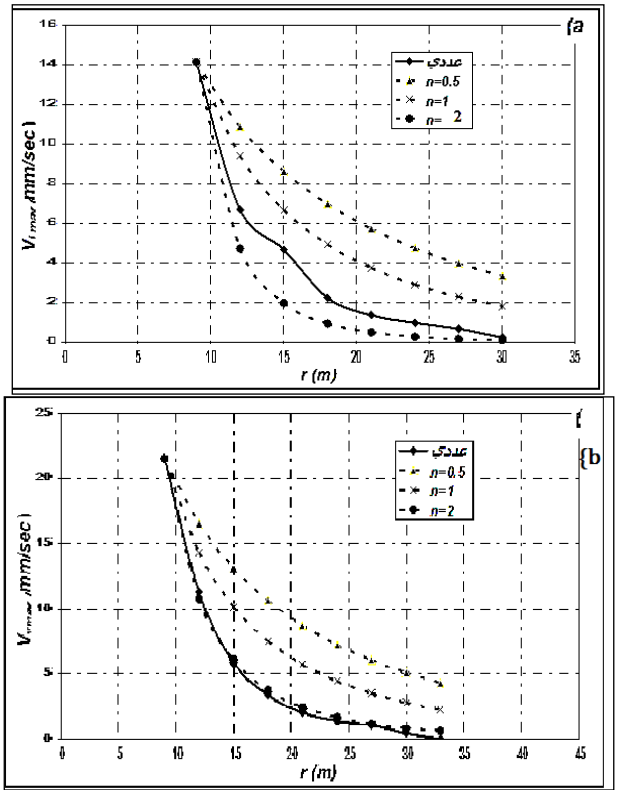

FIGURE (9): CALIBRATION OF THE PORTENEZ DAMPING EQUATION ON THE NUMERICAL DAMPING CURVE WHILE THE CHANGING VALUES OF THE GEOMETRIC DAMPING FACTOR N (FOR A=0).

(A HORIZONTAL VEHICLE V_L (B VERTICAL VEHICLE V_V

We can see from the figure that the physical damping significantly influences the analysis of the results. For example, the numerical damping curve most closely aligns with the curve corresponding to n=2, indicating that the dominant waves in the total vibration time signal are volume waves.

To determine the appropriate value of *n* for use in the previous Bornitz damping relationship when predicting vibration amplitudes resulting from dynamic compaction. Figures (8) and (9) can be re-expressed on a logarithmic scale, which enables the estimation of n equal to the slope of the linear trend curve in this case, as illutrated in the following figure

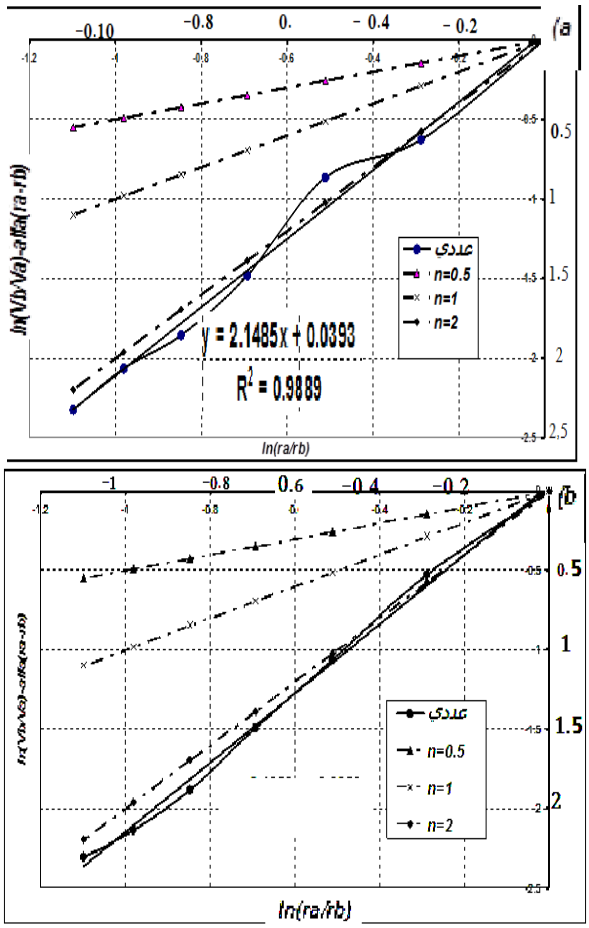

FIGURE (10): LOGARITHMIC REPRESENTATION BASED ON THE PORTENEZ RELATION OF THE VIBRATION DAMPING CURVE CALCULATED AT THE SOIL SURFACE (FOR $A=0.04M^{-1}$):

(A HORIZONTAL VEHICLE V_L (B VERTICAL VEHICLE V_V

From the figure, it can be observed that the value of the geometric damping factor *n* that provides the best approximation to the numerical results, based on the Bornitz relation is n=2.14 for horizontal vibrations and n=2.18 for vertical vibrations.
To further investigate vibration propagation in the frequency domain, the analysis was conducted using a program called MATLAB. We derived the Fourier spectrum curves and determined the value of the dominant frequency, as shown in Figure (11) below.

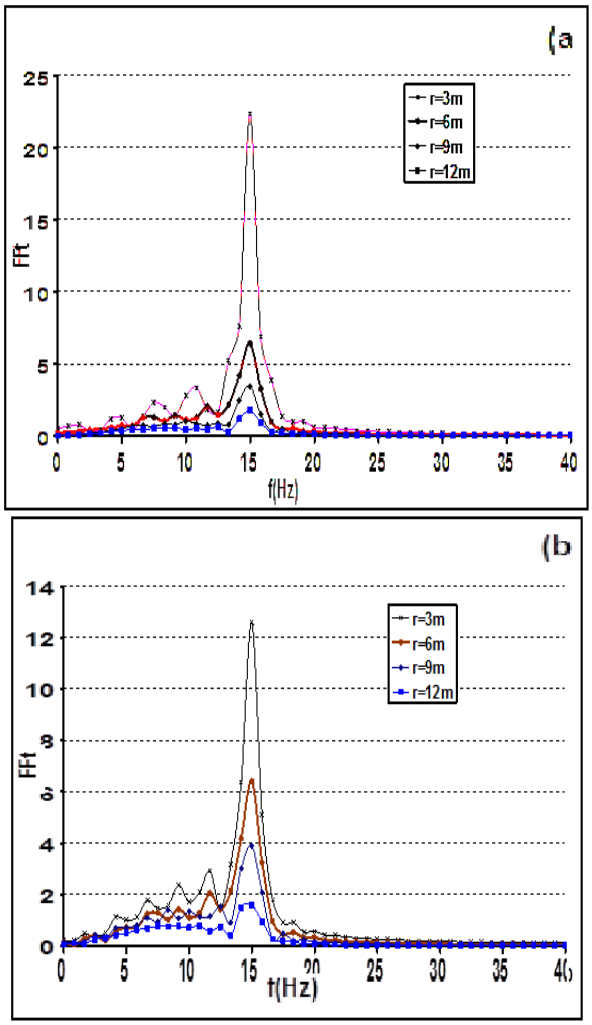

FIGURE (11): COMPARISON OF FOURIER SPECTRA AT VARIOUS DISTANCES FROM THE VIBRATING PROBE.

(B VERTICAL VEHICLE V_V (A HORIZONTAL VEHICLE V_L

From the previous curves, the following observations can be made:
The Fourier spectra of vibrations calculated at different distances along the same direction exhibits the same shape.
The dominant frequency in both the vertical and horizontal directions is 15HZ, which coincides with the excitation frequency of the vibrating probe. used, since the forced frequency is the dominant frequency.
In addition to the vibrations on the soil surface, numerical simulations also enable the investigation of vibration behavior within the soil mass. For instance, Figure (12) illustrates the change in the amplitude of both the horizontal and vertical components

with depth for the vibrations calculated in the vertical sections located at a distance of 12m, 6m from the center of the vibrating probe.
The following figure presents the damping curves for the calculated vibrations within the soil mass for both vertical and horizontal directions.

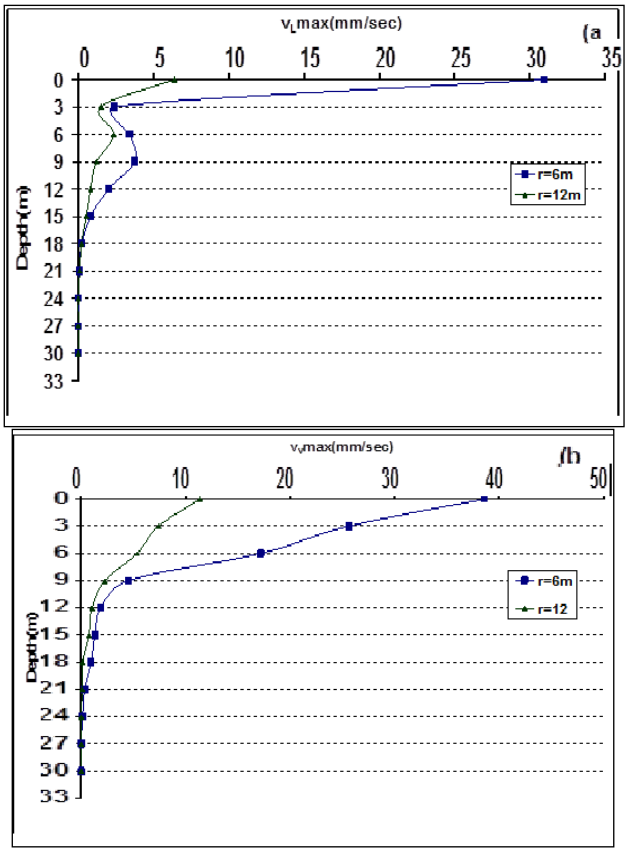

FIGURE (12) : DAMPING CURVES FOR VIBRATIONS CALCULATED WITHIN THE SOIL.

(A HORIZONTAL VEHICLE V_L (B VERTICAL VEHICLE V_V

From the figure the following can be noted:

−The horizontal amplitude of the vibrations at a given distance from the vibrating probe is maximum at the soil surface. It then decreases with depth to approximately 3m, followed by a slight increase reaching a secondary peak at around 9m. Beyond this depth, the amplitude of the horizontal vibrations decreases continuosly until it becomes negligible at a depth of approximately equal $(r = 4.7\lambda_p) \cong 18m$.

- Similarly, the amplitude of the vertical component of the vibrations at a given distance from the vibrating probe is maximum at the soil surface and then decreases continuously with depth until it also reaches a negligible value at a depth of $(r = 6\lambda_p) \cong 18m$

6. Conclusions and recommendations

From this comprehensive study of soil dynamics included by a vibrating probe and the resulting wave amplitudes, the following conclusions can be drawn:

-The vibrations generated by the vibrating probe are due to the propagation of vibration waves within the soil. At a distance of 3 m or more from the vibrating probe, the dominant wave type is the compressional wave P. Identifying the dominant wave type is essential for understanding the mechanisms of energy propagation in the soil, which directly influences the accuracy of the numerical model, its representation of the field conditions, and the reliability of the structural design in deep compaction applications.

-The study enables the prediction of the molecular velocity resulting from the compaction process for a given site. This is critical for mitigating potential risks associated with the dynamic compaction process if the molecular velocity of the vibration exceeds the permissible limits for the studied area. In addition, the model allows prediction of the dominant wave typess when the source of the compaction vibration with the vibrating probe is at specific distances from the source of the vibration.

- The vibration amplitude decreases with increasing distance from the source of vibration according to an exponential relationship of the form factor (correlation factor) R:

$$A.E^{-B.R} = V_{MAX}$$

where a and b are two numerical coefficients. The coefficient a is associated with the amplitude of vibrations near the source of vibrations, while b represents the overall damping (geometric and physical) of vibrations. These coefficients, a and b, were determined in this study based on the type of soil corresponding to the imposed soil parameters. Thus, the components of the vibration amplitude can be determined at any point in the soil. The model enables us to change the soil parameters in accordance with the type of soil under study and to deduce the values of the factors a and b.

-The proposed numerical model provides a practical tool for predicting the generation and propagation of vibration waves both at the surface and within the soil. It enables estimation of potential vibration amplitudes at any location in the soil using the simplified damping relationship.

References

[1] R. D. Anderson, “New method for deep sand vibratory compaction,” *Journal of the Construction Division, ASCE*, vol. 100, no. CO1, pp. 79–95, 1974, doi: 10.1061/JCCEAZ.0000412.

[2] K. R. Massarsch, “Effects of vibratory compaction,” in *TransVib 2002: International Conference on Vibratory Pile Driving and Deep Soil Compaction*, Louvain-la-Neuve, Belgium, 2002, pp. 33–42.

[3] R. D. Woods and L. P. Jedele, “Energy–attenuation relationships from construction vibrations,” in *Vibration Problems in Geotechnical Engineering*, G. Gazetas and E. T. Selig, Eds. New York, NY, USA: ASCE, 1985, pp. 229–246.

[4] H. Amick, T. Xu, and M. Gendreau, “The role of buildings and slabs-on-grade in the suppression of low-amplitude ambient ground vibrations,” in *Proc. 11th*

International Conference on Soil Dynamics and Earthquake Engineering and 3rd International Conference on Earthquake Geotechnical Engineering, Berkeley, CA, USA, Jan. 7–9, 2004, pp. 877–881.

[5] S. Giese, "Numerical simulation of vibroflotation compaction—Application of dynamic boundary conditions," in *Numerical Modeling in Micromechanics via Particle Methods*, H. Konietzky, Ed. Lisse, The Netherlands: A.A. Balkema, 2003, pp. 117–124.

[6] R. D. Woods, "Screening of surface waves in soils," *Journal of the Soil Mechanics and Foundations Division, ASCE*, vol. 94, no. SM4, pp. 951–979, 1968.

[7] M. H. El Naggar and A. G. Chehab, "Vibration barriers for shock-producing equipment," *Canadian Geotechnical Journal*, vol. 42, no. 1, pp. 297–306, 2005, doi: 10.1139/t04-067.

[8] K. R. Massarsch and B. H. Fellenius, "Deep vibratory compaction of granular soils," in *Ground Improvement: Case Histories*, B. Indraratna and J. Chu, Eds. Amsterdam, The Netherlands: Elsevier, 2005, ch. 19, pp. 633–658, doi: 10.1016/S1571-9960(05)80022-9.

[9] K. L. Lee and H. B. Seed, "Drained strength characteristics of sands," *Journal of the Soil Mechanics and Foundations Division, ASCE*, vol. 93, no. SM6, pp. 117–141, 1967, doi: 10.1061/JSFEAQ.0001048.

[10] K. R. Massarsch and B. H. Fellenius, "Vibratory compaction of coarse-grained soils," *Canadian Geotechnical Journal*, vol. 39, no. 3, pp. 695–709, 2002, doi: 10.1139/t02-006.

[11] J. L. Pan and A. R. Selby, "Simulation of dynamic compaction of loose granular soils," *Advances in Engineering Software*, vol. 33, no. 7–10, pp. 631–640, 2002, doi: 10.1016/S0965-9978(02)00067-4.

[12] F. Hage Chehade and I. Shahrour, "Numerical analysis of the interaction between twin-tunnels: Influence of the relative position and construction procedure," *Tunnelling and Underground Space Technology*, vol. 23, no. 2, pp. 210–214, 2008, doi: 10.1016/j.tust.2007.03.004.

[13] K. R. Massarsch, "Man-made vibrations and solutions," in *Proc. Third International Conference on Case Histories in Geotechnical Engineering*, St. Louis, MO, USA, Jun. 1–4, 1993, vol. 2, pp. 1393–1405.

[14] D. Arsenovic, S. B. Vrhovac, Z. M. Jaksic, Lj. Budinski-Petkovic, and A. Belic, "Simulation study of granular compaction dynamics under vertical tapping," *Materials Science Forum*, vol. 555, pp. 107–112, 2007, doi: 10.4028/www.scientific.net/MSF.555.107.

[15] S. Zhai, G. Du, C. Gao, S. Liu, T. Peng, and H. He, "Effect of vibratory probe compaction method on bearing capacity of loess investigated via random finite element analysis," *Soil Dynamics and Earthquake Engineering*, vol. 186, Art. no. 108914, 2024, doi: 10.1016/j.soildyn.2024.108914.